Crystal structures of two polymorphs of alclometasone dipropionate, $C_{28}H_{37}ClO_7$

James A. Kaduk,[1,2,a] Amy M. Gindhart,[3] and Thomas N. Blanton[3]
[1]*Illinois Institute of Technology, 3101 S. Dearborn St., Chicago, Illinois 60616, USA*
[2]*North Central College, 131 S. Loomis St., Naperville, Illinois 60540, USA*
[3]*ICDD, 12 Campus Blvd., Newtown Square, Pennsylvania 19073-3273, USA*

(Received 25 July 2019; accepted 15 December 2019)

The crystal structures of two forms of alclometasone dipropionate have been solved and refined using a single synchrotron X-ray powder diffraction pattern and optimized using density functional techniques. Both forms crystallize in the space group $P2_12_12_1$ (#19) with $Z = 4$. The lattice parameters of Form 1 are $a = 10.44805(7)$, $b = 14.68762(8)$, $c = 17.31713(9)$ Å, and $V = 2657.44(2)$ Å^3, and those of Form 2 are $a = 10.69019(13)$, $b = 14.66136(23)$, $c = 17.17602(23)$ Å, and $V = 2692.05(5)$ Å^3. Both density functional theory and molecular mechanics optimizations indicate that Form 2 is lower in energy, but the differences are within the expected uncertainties of such calculations. In both forms, the only traditional hydrogen bond is between the hydroxyl group and the ketone in the steroid A ring. The chlorine atom acts as an acceptor in two intramolecular C–H···Cl hydrogen bonds involving ring hydrogens, as well as in an intermolecular hydrogen bond involving a methyl group. There are several C–H···O hydrogen bonds, mainly to ketone oxygens, but also to the hydroxyl group and an ether oxygen. The powder patterns have been submitted to ICDD for inclusion in the Powder Diffraction File™. © *2020 International Centre for Diffraction Data.*
[doi:10.1017/S0885715619000940]

Key words: alclometasone dipropionate, Aclovate, powder diffraction, Rietveld refinement, density functional theory

I. INTRODUCTION

Alclometasone dipropionate (original brand name: Aclovate; generic names: Aclosone, Almeta, Delonal, Legederm, Modrasone, Perderm, etc.) is a synthetic steroid used for topical dermatological applications. It is a prodrug, meaning after being administered, it metabolizes into a pharmacologically active drug. Like other topical corticosteroids, alclometasone dipropionate has anti-inflammatory, anti-itching, and vasoconstrictive properties to treat skin dermatoses such as dermatitis (allergic, contact, actinic, etc.), eczema, and psoriasis. Alclometasone dipropionate is insoluble in water and is applied to the skin as a cream (propylene glycol-based solvent) or an ointment (hexylene glycol-based solvent). The IUPAC name (CAS Registry number 66734-13-2) is [2-[(7R,8S,9S,10R,11S,13S,14S,16R,17R)-7-chloro-11-hydroxy-10,13,16-trimethyl-3-oxo-17-propanoyloxy-7,8,9,11,12,14,15,16-octahydro-6H-cyclopenta[a]phenanthren-17-yl]-2-oxoethyl] propanoate. A two-dimensional molecular diagram is shown in Figure 1.

This work was carried out as a part of a project (Kaduk *et al.*, 2014) to determine the crystal structures of large-volume commercial pharmaceuticals and include high-quality powder diffraction data for these pharmaceuticals in the Powder Diffraction File (Fawcett *et al.*, 2017).

[a]Author to whom correspondence should be addressed. Electronic mail: kaduk@polycrystallography.com

II. EXPERIMENTAL

Alclometasone dipropionate was a commercial reagent, purchased from USP (Lot #R044G0), and was used as-received. The white powder was packed into a 1.5 mm diameter Kapton capillary and rotated during the measurement at ~50 Hz. The powder pattern was measured at 295 K at beamline 11-BM (Lee *et al.*, 2008; Wang *et al.*, 2008) of the Advanced Photon Source at Argonne National Laboratory using a wavelength of 0.412826 Å from 0.5 to 50° 2θ with a step size of 0.001° and a counting time of 0.1 s step^{-1}.

The pattern was difficult to index. Difficulty in indexing a high-resolution pattern from 11-BM is a sign that the sample may be a mixture. The strategy that was finally successful was to use DICVOL14 (Louër and Boultif, 2014), allowing up to three unindexed lines and a tolerance of ±0.03°. This yielded a primitive orthorhombic unit cell with $a = 10.5881$, $b = 14.6695$, $c = 17.2491$ Å, $V = 2679.07$ Å^3, and $Z = 4$. Analysis of the systematic absences using EXPO2014 (Altomare *et al.*, 2013) suggested the space group $P2_12_12_1$. A reduced cell search in the Cambridge Structural Database (Groom *et al.*, 2016) combined with the chemistry C, H, Cl, and O only yielded no hits. An alclometasone dipropionate molecule was built using Spartan '18 (Wavefunction, 2018) and converted into .mol2 and .mop files using OpenBabel (O'Boyle *et al.*, 2011). The same structural model was obtained by Monte Carlo simulated annealing techniques using FOX (Favre-Nicolin and Černý, 2002) and EXPO2014.

The initial refinement using GSAS-II (Toby and Von Dreele, 2013) revealed the presence of >13 unindexed

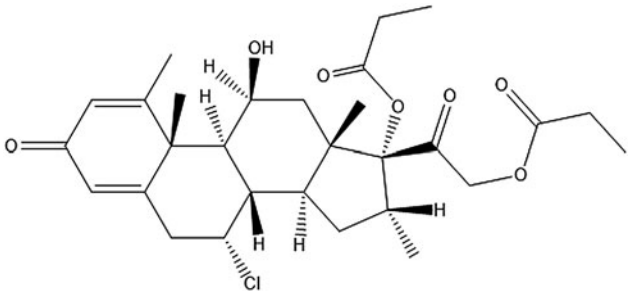

Figure 1. Molecular structure of alclometasone dipropionate.

peaks. These were indexed on a high-quality (M/F = 47.6/415.9) primitive orthorhombic unit cell having $a = 10.6933$, $b = 14.6540$, $c = 17.1724$ Å, and $V = 2690.90$ Å^3 using DICVOL14 (Louër and Boultif, 2014). The similarity of this cell to that of the initial unit cell (defined as Form 1 alclometasone dipropionate) led us to modify that cell and carry out a molecular mechanics geometry optimization using the Forcite module of Materials Studio (Dassault, 2018) to obtain an initial structural model for what was defined as Form 2 alclometasone dipropionate. The final refinement was begun using the results from the density functional theory (DFT) calculations.

The Rietveld refinement was carried out using GSAS-II (Toby and Von Dreele, 2013). Only the 2.0–20.0° portion of the pattern was included in the refinement ($d_{min} = 1.188$ Å). All non-H bond distances and angles were subjected to restraints, based on a Mercury/Mogul Geometry Check (Bruno *et al.*, 2004; Sykes *et al.*, 2011) of the molecule. The results were exported to a csv file. The Mogul average and standard deviation for each quantity were used as the restraint parameters and were incorporated using the new feature Restraints/Edit Restraints/Add MOGUL Restraints, which reads the bond distance and angle restraints from the csv file. The restraints contributed 4.2% to the final χ^2. The hydrogen atoms were included in calculated positions, which were

TABLE I. Root-mean-square Cartesian displacements (Å) between the two polymorphs of alclometasone dipropionate.

	Form 1 Rietveld	Form 1 DFT	Form 2 Rietveld	Form 2 DFT
Form 1 Rietveld	–	0.131	0.428	0.158
Form 1 DFT		–	0.372	0.225
Form 2 Rietveld			–	0.459
Form 2 DFT				–

recalculated during the refinement using Materials Studio (Dassault, 2018). A common U_{iso} was refined for the non-H atoms of the ring system of Form 1 and another for the non-H atoms of the side chains. The U_{iso} of these atoms in Form 2 were fixed to the values of Form 1. The U_{iso} for each hydrogen atom was constrained to be 1.3× that of the heavy atom to which it is attached. The background was modeled using a 3-term shifted Chebyshev polynomial, and a peak at 5.26° to model the scattering from the Kapton capillary and any amorphous component.

The final refinement of 245 variables using 18 029 observations and 202 restraints yielded the residuals Rwp = 0.0852 and GOF = 1.33. The largest peak (1.64 Å from C67) and hole (1.60 Å from O66) in the difference Fourier map for Form 1 were 0.36 and −0.38(9) eÅ^{-3}, and the largest peak (0.10 Å from C17) and hole (1.75 Å from O51) in the difference Fourier map for Form 2 were 0.38 and −0.45(11) eÅ^{-3}, respectively. The Rietveld plot is included in Figure 2. The largest errors in the fit are in the shapes of some of the strong low-angle peaks and in the description of the amorphous background.

Density functional geometry optimizations were carried out for both forms using CRYSTAL14 (Dovesi *et al.*, 2014). The basis sets for the H, C, N, and O atoms were those of Gatti *et al.* (1994), and the basis set for Cl was that of Peintinger *et al.* (2013). The calculations were run on

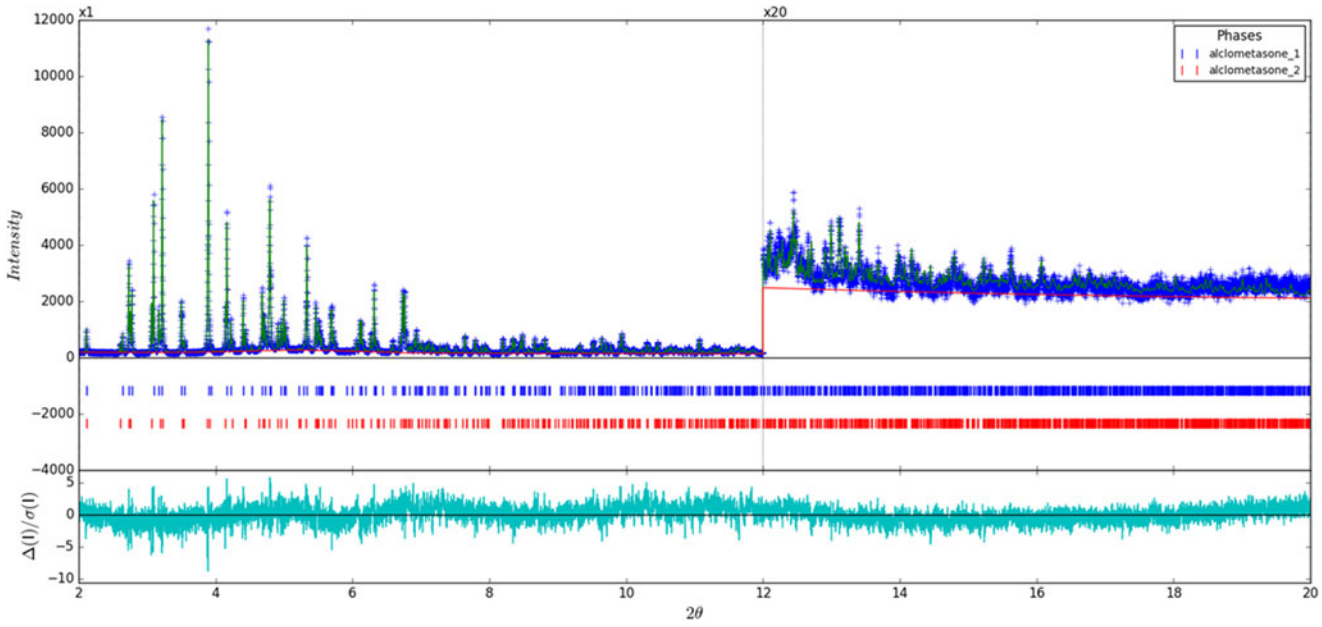

Figure 2. (Color online) Rietveld plot for the refinement of alclometasone dipropionate present in both Form 1 and Form 2. The blue crosses represent the observed data points, and the green line is the calculated pattern. The cyan curve is the normalized error plot. The vertical scale has been multiplied by a factor of 20× for 2θ> 12°.

https://doi.org/10.1017/S0885715619000940 Published online by Cambridge University Press

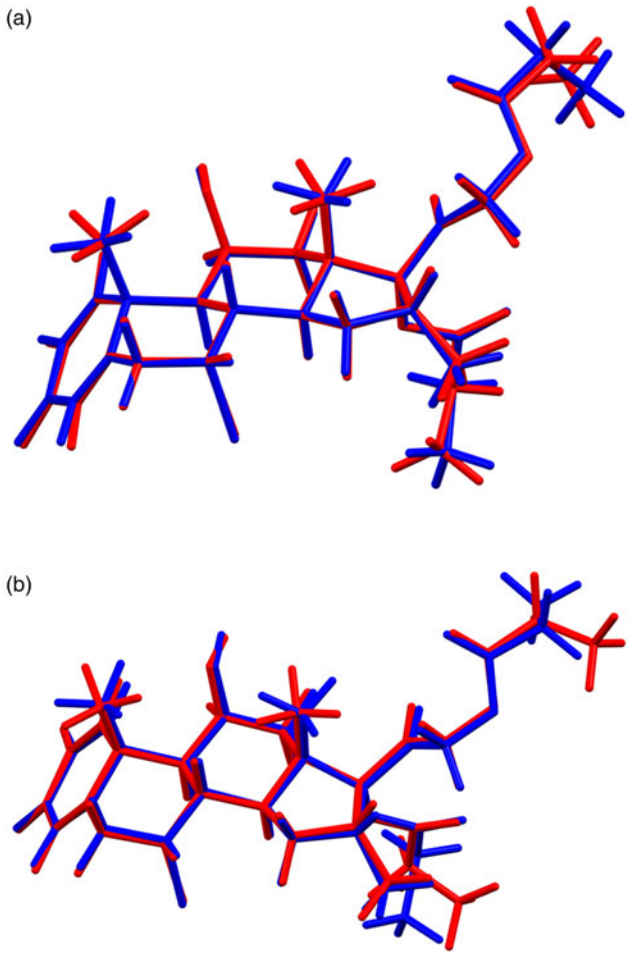

Figure 3. (Color online) (a) Comparison of the Rietveld-refined (red) and CRYSTAL14-optimized (blue) structures of alclometasone dipropionate, Form 1. (b) Comparison of the Rietveld-refined (red) and CRYSTAL14-optimized (blue) structures of alclometasone dipropionate, Form 2.

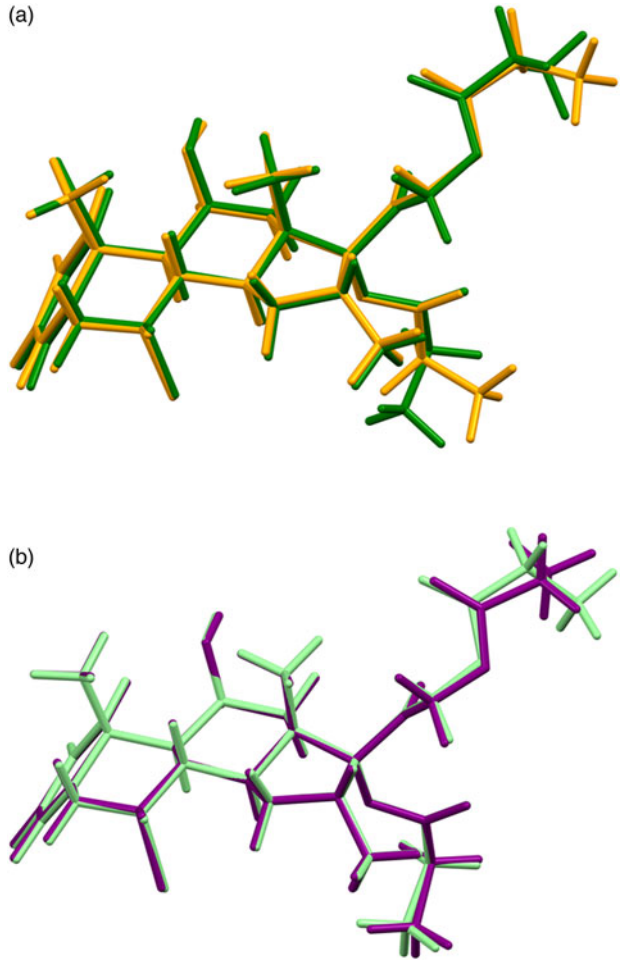

Figure 4. (Color online) (a) Comparison of the Rietveld-refined structures of alclometasone dipropionate Form 1 (green) and Form 2 (orange). (b) Comparison of the CRYSTAL14-optimized structures of alclometasone dipropionate Form 1 (light green) and Form 2 (purple).

eight 2.1 GHz Xeon cores (each with 6 GB RAM) of a 304-core Dell Linux cluster at IIT, using 8 *k*-points and the B3LYP functional, and took ∼175 h (Form 1) and ∼123 h (Form 2).

III. RESULTS AND DISCUSSION

The refined atom coordinates of both forms of alclometasone dipropionate and the coordinates from the DFT optimizations are reported in the CIFs deposited with ICDD. The root-mean-square Cartesian displacements of the two forms are compared in Table I. The agreement between the refined and optimized structures of Form 1 is excellent [Figure 3(a)], confirming that the structure is correct (van de Streek and Neumann, 2014). The largest difference is at C61, the methyl group at the end of one propionate side chain. The agreement between the refined and optimized structures of Form 2 is not as good as observed for Form 1 [Figure 3(b)] and reflects differences in the conformations of both methyl groups C61 and C70 at the ends of the propionate side chains. The Form 2 polymorph is a minority phase (32.0(2) wt%) and is probably determined less accurately than Form 1. The largest differences between the Rietveld-refined structures of the two forms are at both methyl groups C61 and C70 [Figure 4(a)], while the DFT-optimized structures differ mainly at C61 [Figure 4(b)]. This discussion concentrates on the CRYSTAL-optimized structures. The asymmetric units (with the atom numbering) are illustrated in Figure 5(a), Form 1 and Figure 5(b), Form 2; and the crystal structures are presented in Figure 6(a), Form 1 and Figure 6(b), Form 2.

The two structures are nearly identical (Figure 7). The differences lie in the orientations of the methyl groups C61 at the ends of the propionate side chains and in subtle differences in the hydrogen bonds. The propionate side chains may be disordered. The general orientation of the molecules is in the *ac*-plane. The solid-state DFT calculations indicate that Form 2 is lower in energy by −0.04 kcal mol^{-1}. The energy difference is well within the expected uncertainty of such calculations, so the two forms must be considered equivalent in energy. Compared to those of Form 1, the lattice parameters of Form 2 differ by +2.32%, −0.18%, and −0.82%, respectively; the cell volume of Form 2 is 1.30% larger than that of Form 1.

All of the bond distances and angles in both forms fall within the normal ranges indicated by a Mercury–Mogul Geometry Check (Macrae *et al.*, 2008). In both forms, the torsion angles involving rotation about the C40–C50 bond lie on the tails of the expected distributions or in minority populations. In Form 2, the O49–C65–C67–C70 torsion angle is flagged as unusual. These torsion angles reflect the

https://doi.org/10.1017/S0885715619000940 Published online by Cambridge University Press

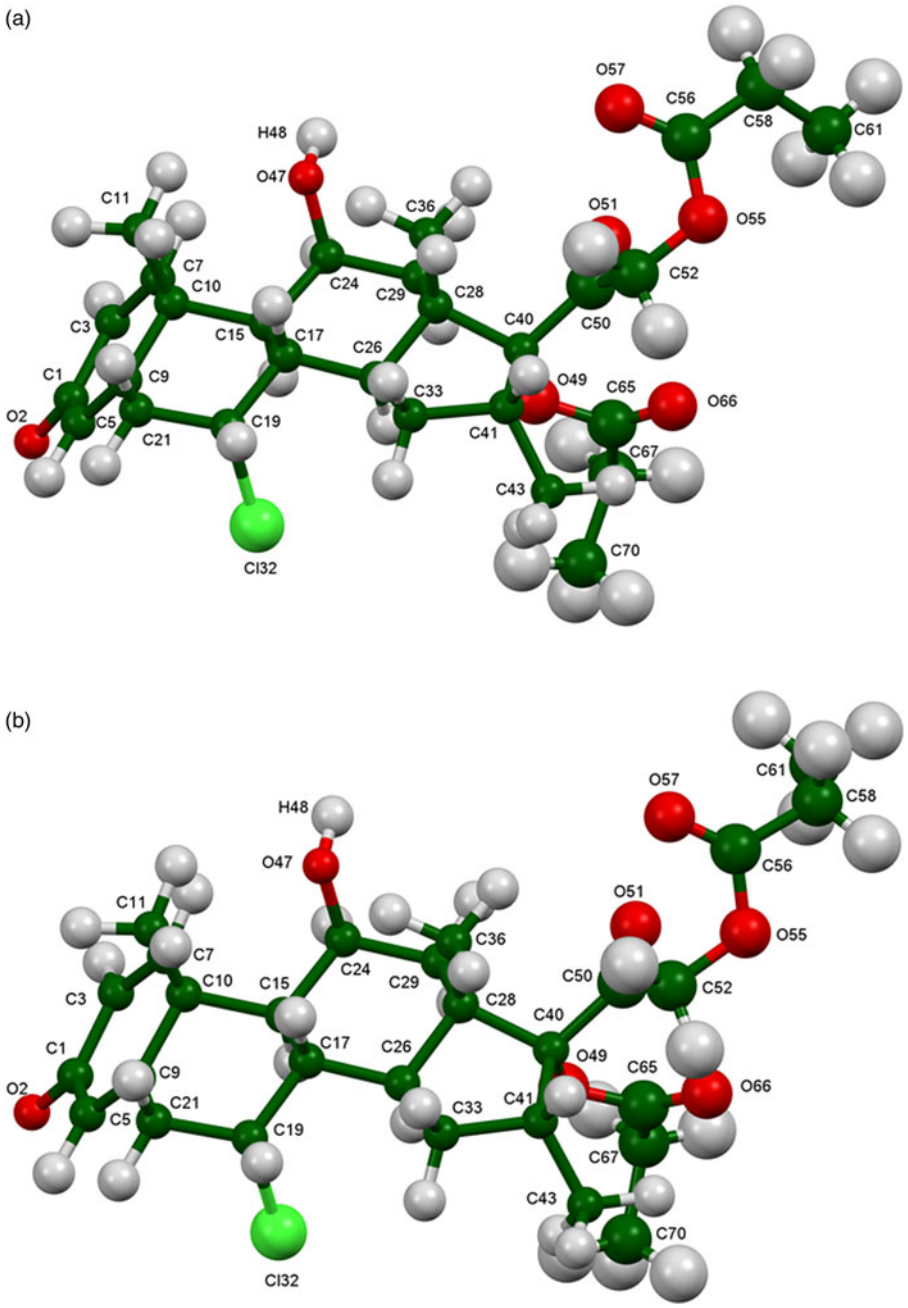

Figure 5. (Color online) (a) Asymmetric unit of alclometasone dipropionate, Form 1, with the atom numbering. The atoms are represented by 50% probability spheroids. (b) Asymmetric unit of alclometasone dipropionate, Form 2, with the atom numbering. The atoms are represented by 50% probability spheroids.

orientations of the propionate side chains with respect to the steroid core. Presumably, molecular crowding results in unusual conformations. The O55–C56–C58–C61 torsion angle in Form 2 is also flagged as unusual. The two propionate chains in both forms have different conformations (Table II). Even though the O55–C56–C58–C61 and O49–C65–C67–C70 torsion angles in Form 2 are flagged as unusual and the comparable torsions in Form 1 are not; in both forms, these torsion angles lie in the extended tail of a distribution around the normal value of ∼180° [Figures 8(a) and 8(b)]. This observation points out the importance of actually looking at the distributions of torsion angles.

Quantum chemical geometry optimizations (DFT/B3LYP/6-31G*/water) using Spartan ‘18 (Wavefunction, 2018) indicated that the conformation of molecule 2 is 0.1 kcal mol^{-1} lower in energy than that of molecule 1, and thus that the energies are indistinguishable. The minimum energy conformation has a third arrangement of the methyl groups at the ends of the propionate chains, which suggests that these chains may be flexible and/or disordered.

The analysis of the contributions to the total crystal energy in both forms using the Forcite module of Materials Studio (Dassault, 2018) indicates that Form 2 is also slightly lower in energy, and suggests that bond and angle distortion terms are significant in the intramolecular deformation energy, as might be expected for a fused-ring system. The intermolecular energy is dominated by electrostatic attractions, which in this force-field-based analysis include hydrogen bonds. The hydrogen bonds are better analyzed using the results of the DFT calculations.

https://doi.org/10.1017/S0885715619000940 Published online by Cambridge University Press

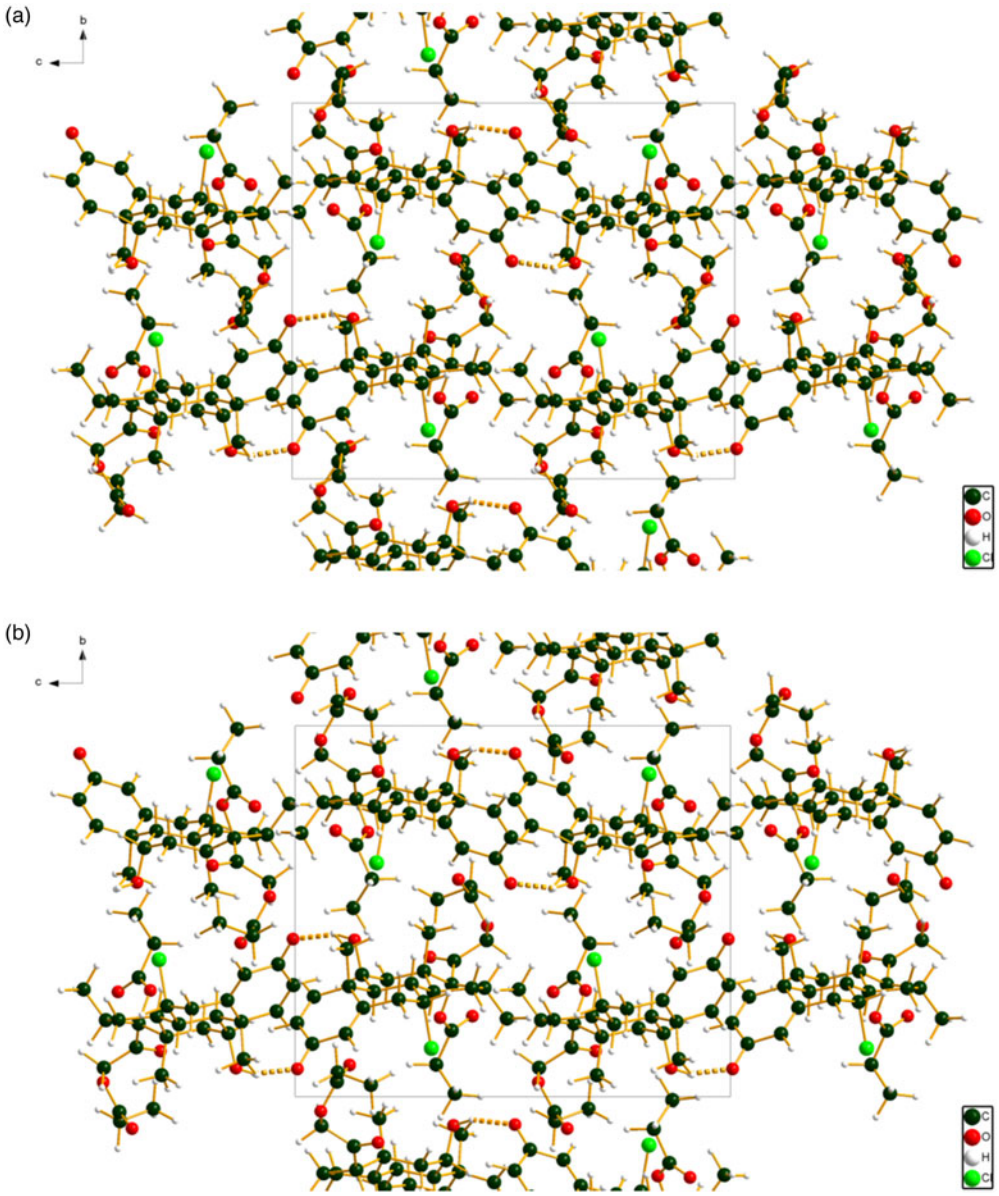

Figure 6. (Color online) (a) Crystal structure of alclometasone dipropionate, Form 1, viewed down the *a*-axis. (b) Crystal structure of alclometasone dipropionate, Form 2, viewed down the *a*-axis.

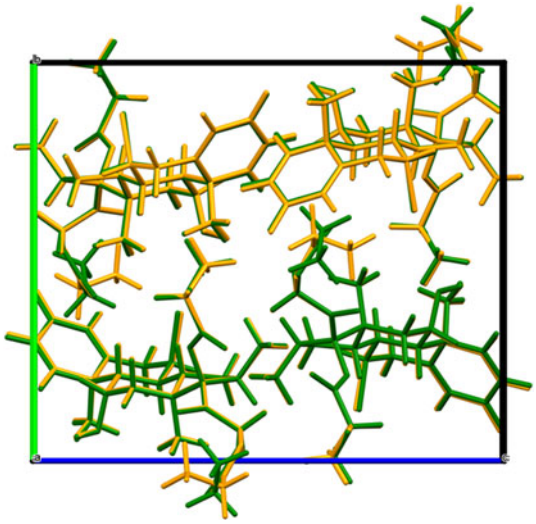

Figure 7. (Color online) Comparison of Form 1 (green) and Form 2 (orange) alclometasone dipropionate structures.

The H-bond landscape is surprisingly rich (Tables III and IV). In both forms, the only traditional hydrogen bond is between the hydroxyl group O47 and the ketone O2. These discrete hydrogen bonds link pairs of molecules along the *c*-axis. The energies of these hydrogen bonds were calculated using the correlation of Rammohan and Kaduk (2018). In both forms, Cl32 acts as an acceptor in two intramolecular

TABLE II. Propionate torsion angles (°) in the DFT-optimized structures of the two polymorphs of alclometasone dipropionate.

Polymorph	Form 1	Form 2
C50–C52–O55–C56	81.0	84.7
C52–O55–C56–C58	171.2	−172.6
O55–C56–C58–C61	23.8	94.1
C28–C40–O49–C65	158.8	158.1
C40–O49–C65–C67	179.8	−178.5
O49–C65–C67–C70	−76.5	−83.2

https://doi.org/10.1017/S0885715619000940 Published online by Cambridge University Press

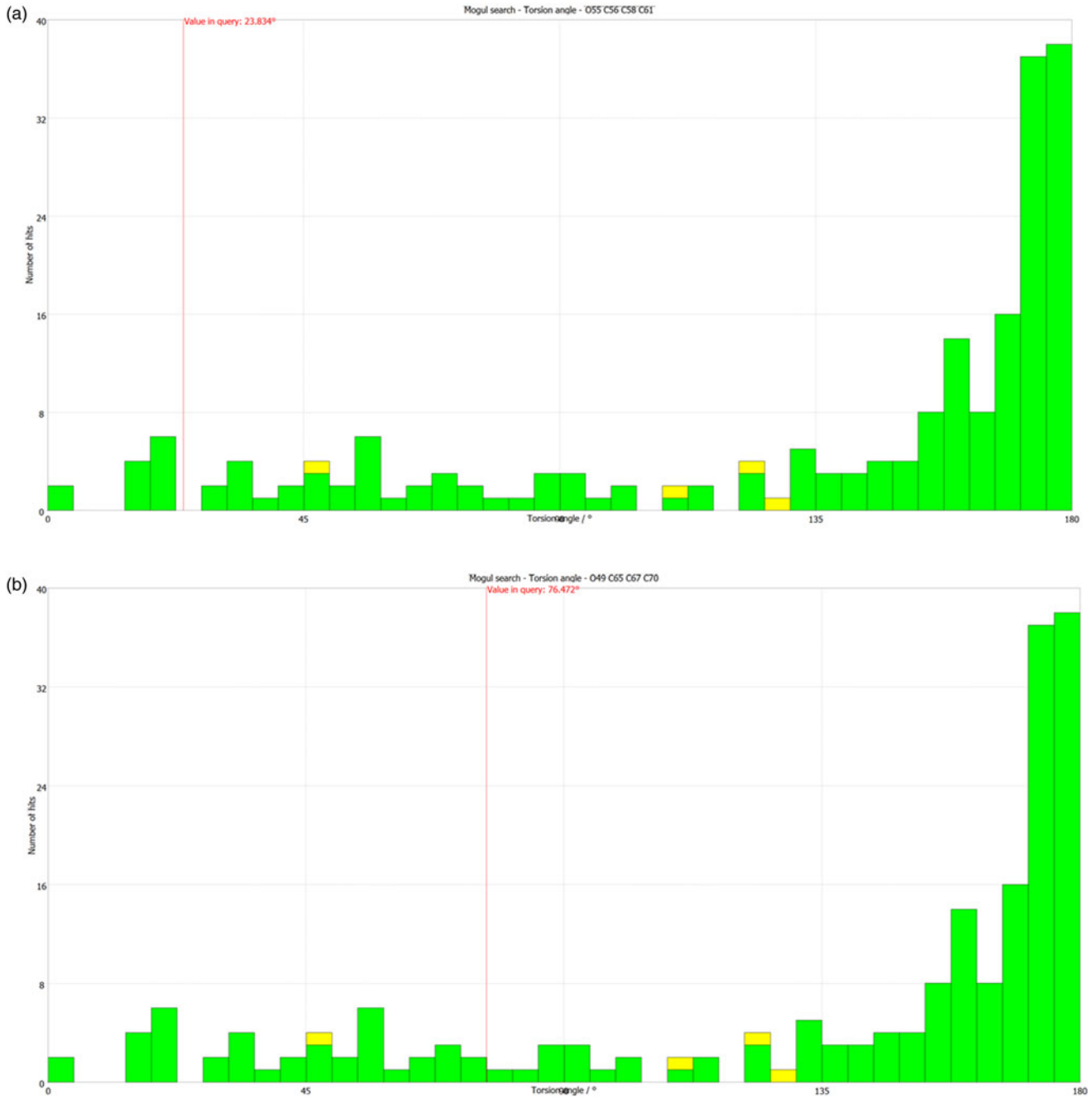

Figure 8. (Color online) (a) The "not unusual" O55–C56–C58–C61 torsion angle in alclometasone dipropionate Form 1 compared to the Mogul distribution of similar torsion angles. (b) The "unusual" O49–C65–C67–C70 torsion angle in alclometasone dipropionate Form 1 compared to the Mogul distribution of similar torsion angles.

TABLE III. Hydrogen bonds (CRYSTAL14) in alclometasone dipropionate Form 1.

H-bond	D-H (Å)	H···A (Å)	D···A (Å)	D-H···A (°)	Overlap (*e*)	*E* (kcal mol^{-1})
O47–H48···O2	0.976	1.840	2.758	155.7	0.045	11.6
C26–H27···Cl32	1.097	2.678[a]	3.117	103.2	0.017	
C15–H16···Cl32	1.098	2.940[a]	3.424	106.9	0.011	
C36–H38···Cl32	1.088	2.865	3.809	145.1	0.010	
C70–H71···O51	1.093	2.610	3.560	145.0	0.009	
C67–H68···O57	1.094	2.305	3.395	174.0	0.020	
C52–H54···O57	1.096	2.413[a]	2.691	92.4	0.012	
C52–H54···O2	1.096	2.682	3.753	165.3	0.017	
C43–H44···O66	1.089	2.252	3.203	144.6	0.016	
C29–H30···O49	1.093	2.304	2.782	104.2	0.009	
C11–H14···O47	1.087	2.280[a]	2.899	101.0	0.017	
C5–H6···O57	1.085	2.441	3.415	148.7	0.014	
C36–H39···C50	1.093	2.556[a]	2.863	94.8	0.011	

[a]Intramolecular.

https://doi.org/10.1017/S0885715619000940 Published online by Cambridge University Press

TABLE IV. Hydrogen bonds (CRYSTAL14) in alclometasone dipropionate Form 2.

H-bond	D-H (Å)	H···A (Å)	D···A (Å)	D-H···A (°)	Overlap (*e*)	*E* (kcal mol^{-1})
O47–H48···O2	0.976	1.848	2.763	155.2	0.045	11.6
C26–H27···Cl32	1.097	2.703[a]	3.124	102.2	0.016	
C36–H38···Cl32	1.097	2.882	3.806	142.8	0.009	
C15–H16···Cl32	1.098	2.992[a]	3.452	105.6	0.007	
C70–H73···O51	1.093	2.679	3.605	142.1	0.008	
C67–H68···O57	1.093	2.374	3.455	169.8	0.019	
C52–H54···O57	1.097	2.427[a]	2.714	93.0	0.012	
C52–H54···O2	1.097	2.550	3.608	161.8	0.021	
C43–H46···O66	1.090	2.303	3.251	144.3	0.016	
C29–H30···O49	1.094	2.320	2.788	103.6	0.009	
C11–H14···O47	1.087	2.291[a]	2.891	112.7	0.017	
C5–H6···O57	1.085	2.542	3.494	145.8	0.013	
C36–H39···C50	1.093	2.563[a]	2.862	94.4	0.010	

[a]Intramolecular.

C–H···Cl hydrogen bonds involving the ring hydrogens H16 and H27, as well as in an intermolecular hydrogen bond involving the methyl group C36–H38. There are several C–H···O hydrogen bonds, mainly to ketone oxygens, but also to the hydroxyl group O47 and the ether oxygen O49. There is also an intramolecular C–H···C hydrogen bond from the methyl group C36 to the ketone carbon C50. The topologies of the hydrogen bonds in the two forms are the same, but the strengths differ subtly.

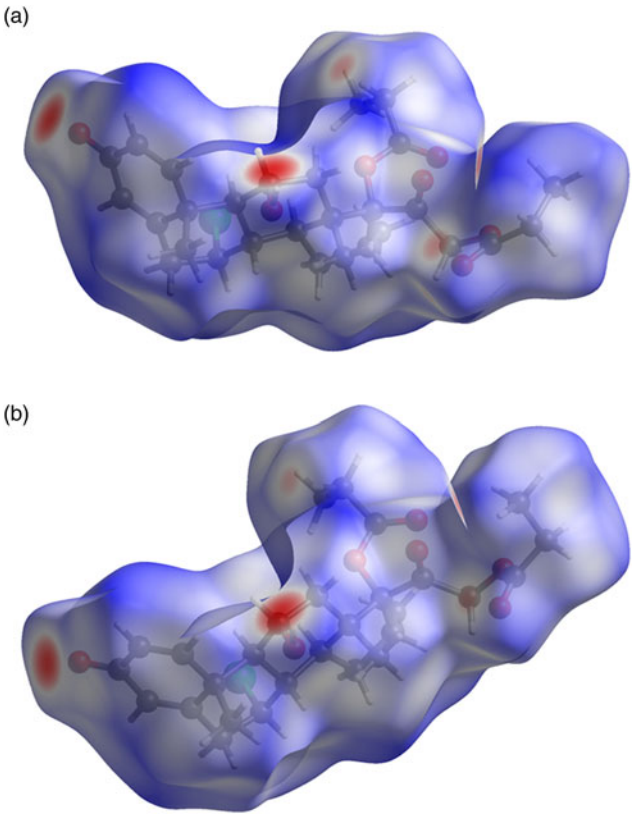

Figure 9. (Color online) (a) Hirshfeld surface of alclometasone dipropionate, Form 1. Intermolecular contacts longer than the sums of the van der Waals radii are colored blue, and contacts shorter than the sums of the radii are colored red. Contacts equal to the sums of radii are white. (b) Hirshfeld surface of alclometasone dipropionate, Form 2. Intermolecular contacts longer than the sums of the van der Waals radii are colored blue, and contacts shorter than the sums of the radii are colored red. Contacts equal to the sums of radii are white.

The volumes enclosed by the Hirshfeld surfaces (Figure 9; Hirshfeld, 1977; Turner, *et al.*, 2017) of Form 1 and Form 2 are 655.63 and 664.06 Å^3, 98.68% and 98.67% of 1/4 the unit cell volumes, respectively. The molecules, thus, exhibit typical packing density. All of the significant close contacts (red in Figure 9) involve the hydrogen bonds. The volume/non-H atom is 18.4 and 18.7 Å^3.

The Bravais–Friedel–Donnay–Harker (Bravais, 1866; Friedel, 1907; Donnay and Harker, 1937) morphology suggests that we might expect blocky morphology for alclometasone dipropionate. The second-order spherical harmonic models were included in the refinement. The texture indices were 1.001 and 1.008, indicating that the preferred orientation was not significant in this rotated capillary specimen. The powder patterns of the two forms of alclometasone dipropionate from this synchrotron data set have been submitted to ICDD for inclusion in the Powder Diffraction File™.

DEPOSITED DATA

CIF and/or RAW data files were deposited with ICDD. You may request this data from ICDD at info@icdd.com.

ACKNOWLEDGEMENTS

We thank Lynn Ribaud and Saul Lapidus for their assistance in the data collection, and Andrey Rogachev for the use of computing resources at IIT.

FUNDING INFORMATION

The use of the Advanced Photon Source at Argonne National Laboratory was supported by the U.S. Department of Energy, Office of Science, Office of Basic Energy Sciences, under Contract No. DE-AC02-06CH11357. This work was partially supported by the International Centre for Diffraction Data.

CONFLICTS OF INTEREST

The authors have no conflicts of interest to declare.

Altomare, A., Cuocci, C., Giacovazzo, C., Moliterni, A., Rizzi, R., Corriero, N., and Falcicchio, A. (**2013**). "EXPO2013: a kit of tools for phasing crystal structures from powder data," J. Appl. Crystallogr. **46**, 1231–1235.

https://doi.org/10.1017/S0885715619000940 Published online by Cambridge University Press

Bravais, A. (**1866**). *Etudes Cristallographiques* (Gauthier Villars, Paris).
Bruno, I. J., Cole, J. C., Kessler, M., Luo, J., Motherwell, W. D. S., Purkis, L. H., Smith, B. R., Taylor, R., Cooper, R. I., Harris, S. E., and Orpen, A. G. (**2004**). "Retrieval of crystallographically-derived molecular geometry information," J. Chem. Inf. Comput. Sci. **44**, 2133–2144.
Dassault Systèmes (**2018**). *Materials Studio 2019* (BIOVIA, San Diego, CA).
Donnay, J. D. H. and Harker, D. (**1937**). "A new law of crystal morphology extending the law of Bravais," Am. Mineral. **22**, 446–447.
Dovesi, R., Orlando, R., Erba, A., Zicovich-Wilson, C. M., Civalleri, B., Casassa, S., Maschio, L., Ferrabone, M., De La Pierre, M., D-Arco, P., Noël, Y., Causà, M., and Kirtman, B. (**2014**). "CRYSTAL14: A program for the ab initio investigation of crystalline solids," Int. J. Quantum Chem. **114**, 1287–1317.
Favre-Nicolin, V. and Černý, R. (**2002**). "FOX, 'Free objects for crystallography': a modular approach to ab initio structure determination from powder diffraction," J. Appl. Crystallogr. **35**, 734–743.
Fawcett, T. G., Kabekkodu, S. N., Blanton, J. R., and Blanton, T. N. (**2017**). "Chemical analysis by diffraction: the Powder Diffraction File™," Powder Diffr. **32**(2), 63–71.
Friedel, G. (**1907**). "Etudes sur la loi de Bravais," Bull. Soc. Fr. Mineral. **30**, 326–455.
Gatti, C., Saunders, V. R., and Roetti, C. (**1994**). "Crystal-field effects on the topological properties of the electron-density in molecular crystals - the case of urea," J. Chem. Phys. **101**, 10686–10696.
Groom, C. R., Bruno, I. J., Lightfoot, M. P., and Ward, S. C. (**2016**). "The Cambridge structural database," Acta Crystallogr. Sect. B: Struct. Sci., Cryst. Eng. Mater. **72**, 171–179.
Hirshfeld, F. L. (**1977**). "Bonded-atom fragments for describing molecular charge densities," Theor. Chem. Acta. **44**, 129–138.
Kaduk, J. A., Crowder, C. E., Zhong, K., Fawcett, T. G., and Suchomel, M. R. (**2014**). "Crystal structure of atomoxetine hydrochloride (Strattera), $C_{17}H_{22}NOCl$," Powder Diffr. **29**(3), 269–273.
Lee, P. L., Shu, D., Ramanathan, M., Preissner, C., Wang, J., Beno, M. A., Von Dreele, R. B., Ribaud, L., Kurtz, C., Antao, S. M., Jiao, X., and Toby, B. H. (**2008**). "A twelve-analyzer detector system for high-resolution powder diffraction," J. Synch. Rad. **15**(5), 427–432.
Louër, D. and Boultif, A. (**2014**). "Some further considerations in powder diffraction pattern indexing with the dichotomy method," Powder Diffr. **29**, S7–S12.
Macrae, C. F., Bruno, I. J., Chisholm, J. A., Edington, P. R., McCabe, P., Pidcock, E., Rodriguez-Monge, L., Taylor, R., van de Streek, J., and Wood, P. A. (**2008**). "Mercury CSD 2.0 – new features for the visualization and investigation of crystal structures," J. Appl. Crystallogr. **41**, 466–470.
O'Boyle, N., Banck, M., James, C. A., Morley, C., Vandermeersch, T., and Hutchison, G. R. (**2011**). "Open Babel: an open chemical toolbox," J. Chem. Informatics **3**, 33.
Peintinger, M. F., Vilela Oliveira, D., and Bredow, T. (**2013**). "Consistent Gaussian basis sets of triple-zeta valence with polarization quality for solid-state calculations," J. Comput. Chem. **34**, 451–459.
Rammohan, A. and Kaduk, J. A. (**2018**). "Crystal structures of alkali metal (Group 1) citrate salts," Acta Cryst. Sect. B: Cryst. Eng. Mater. **74**, 239–252.
Sykes, R. A., McCabe, P., Allen, F. H., Battle, G. M., Bruno, I. J., and Wood, P. A. (**2011**). "New software for statistical analysis of Cambridge Structural Database data," J. Appl. Crystallogr. **44**, 882–886.
Toby, B. H. and Von Dreele, R. B. (**2013**). "GSAS II: the genesis of a modern open source all purpose crystallography software package," J. Appl. Crystallogr. **46**, 544–549.
Turner, M. J., McKinnon, J. J., Wolff, S. K., Grimwood, D. J., Spackman, P. R., Jayatilaka, D., and Spackman, M. A. (**2017**). *CrystalExplorer17* (University of Western Australia). Available at: http://hirshfeldsurface.net.
van de Streek, J. and Neumann, M. A. (**2014**). "Validation of molecular crystal structures from powder diffraction data with dispersion-corrected density functional theory (DFT-D)," Acta Cryst. Sect. B: Struct. Sci., Cryst. Eng. Mater. **70**(6), 1020–1032.
Wang, J., Toby, B. H., Lee, P. L., Ribaud, L., Antao, S. M., Kurtz, C., Ramanathan, M., Von Dreele, R. B., and Beno, M. A. (**2008**). "A dedicated powder diffraction beamline at the Advanced Photon Source: Commissioning and early operational results," Rev. Sci. Inst. **79**, 085105.
Wavefunction, Inc. (**2018**). Spartan '18 Version 1.2.0 (Wavefunction Inc., Irvine, CA).

https://doi.org/10.1017/S0885715619000940 Published online by Cambridge University Press